

ORDER, DISORDER, AND PHASE TRANSITION  
IN CONDENSED SYSTEMS

# Magnetoresistance Hysteresis in Granular HTSCs as a Manifestation of the Magnetic Flux Trapped by Superconducting Grains in YBCO + CuO Composites

D. A. Balaev\*, D. M. Gokhfeld, A. A. Dubrovskii, S. I. Popkov,  
K. A. Shaikhutdinov, and M. I. Petrov

Kirenskii Institute of Physics, Siberian Branch, Russian Academy of Sciences, Krasnoyarsk, 660036 Russia

\* e-mail: smp@iph.krasn.ru

Received February 7, 2007

**Abstract**—Hysteretic behavior of the magnetoresistance of granular HTSCs and its interaction with the magnetic hysteresis are studied by measuring magnetoresistance  $R(H)$  and critical current  $I_c(H)$  of composites formed by HTSC  $Y_{0.75}Lu_{0.25}Ba_2Cu_3O_7$  and CuO. A network of Josephson junctions is formed in such composites, in which the nonsuperconducting component plays the role of barriers between HTSC grains. Hysteretic dependences  $R(H)$  of magnetoresistance are studied in a wide range of transport current density  $j$  and are analyzed in the framework of the two-level model of a granular superconductor, in which dissipation takes place in the Josephson medium and the magnetic flux can be pinned both in grains and in the Josephson medium. The interrelation between the hysteresis of critical current  $I_c(H)$  and the evolution of the hysteretic dependence  $R(H)$  of the magnetoresistance upon transport current variation is demonstrated experimentally. The effect of the magnetic past history on the hysteretic behavior of  $R(H)$  and the emergence of a segment with a negative magnetoresistance are analyzed. It is shown for the first time that the  $R(H)$  dependences are characterized by a parameter that is independent of the transport current, viz., the width of the  $R(H)$  hysteresis loop.

PACS numbers: 74.81.Fa, 74.50.+r

DOI: 10.1134/S1063776107120084

## 1. INTRODUCTION

In spite of the fact that the main features of galvanomagnetic effects in granular high-temperature superconductors (HTSCs) were revealed soon after the discovery of these materials [1–17], the interest in this research has not faded (see recent publications [18–32]). This is due to the fact that the physical mechanisms leading to well-known experimental facts such as the field hysteresis of critical current  $I_c(H)$  [3, 5, 19, 22] and magnetoresistance  $R(H)$  [2–4, 8, 10, 13–15, 18, 20–22, 25], as well as the existence of extrema on the  $I_c(H)$  and  $R(H)$  dependence upon a decrease in the external magnetic field [3, 5, 22] and nonzero residual resistance [3, 10–13, 15, 18, 22, 25], have not been revealed and are not completely clear.

The boundaries between superconducting crystallites in granular HTSCs form a branched network of weak bonds of the Josephson type. When transport current flows through such a network, the resistive state is primarily determined by grain boundaries. The network of Josephson junctions can be described as a Josephson medium that behaves like a type II superconductor [33]. The magnetic flux can exist and be pinned in both subsystems (in grains and in intercrystallite boundaries) [15, 16, 18, 22, 33, 34].

The forms of the hysteretic dependence  $R(H)$  of the magnetoresistance in granular HTSCs are diversified [2–4, 10, 13, 18, 20–22, 25]. As a rule, the  $R(H)$  dependences are measured under the conditions when the value of transport current density  $j$  is lower than the critical value ( $j < j_c$ ). No information has been obtained on the conditions in which the reverse branch of the  $R(H)$  dependence contains a segment with zero resistance or acquires a minimum and a residual resistance, nor on a parameter that can characterize the hysteresis in  $R(H)$ . It remains unclear whether the  $R(H)$  hysteresis is caused by pinning of Abrikosov vortices in superconducting grains or by pinning of vortices in the Josephson medium [15, 18, 22, 29].

To obtain reliable experimental information on magnetoresistance hysteresis, a wider range of transport current density should be used both below the critical value and above it (in zero external field). This is difficult to attain in experiments with polycrystalline HTSCs in view of high values of the measuring current even at liquid nitrogen temperature. For this reason, it is expedient to study granular HTSCs in which Josephson junctions are obviously suppressed, while the properties of superconducting grains remain the same as in HTSC polycrystals. Such objects are HTSC-based composites [35–40].

In this study, we analyze hysteretic dependences of the magnetoresistance and critical current in  $Y_{0.75}Lu_{0.25}Ba_2Cu_3O_7$  composites<sup>1</sup> and CuO. The addition of CuO in amounts of 30 and 15 vol % leads to a decrease in the critical current density  $j_c$  (4.2 K) of the composite to 0.5–20 A/cm<sup>2</sup>. This makes it possible to measure the magnetoresistance at a temperature of 4.2 K for  $j \ll j_c$  (composite with 15 vol % CuO) as well as for  $j \sim j_c$  and  $j > j_c$  (composite with 30 vol % CuO) using relatively weak measuring currents, which makes it possible to avoid sample heating. It was shown earlier from analysis of the current–voltage ( $IV$ ) characteristics and temperature dependences of the resistance that  $Y_{0.75}Lu_{0.25}Ba_2Cu_3O_7 + CuO$  composites have the form of a network of Josephson junctions, in which the non-superconducting component plays the role of Josephson barriers between HTSC crystallites [30, 37, 38]. Consequently, the composites can be treated as a “model” granular HTSC with “strong” superconducting grains (“banks”) and extended intercrystallite boundaries (weak bonds) [37, 38].

This study aims at establishing the interrelation between the hysteretic dependences of the critical current, magnetoresistance, and magnetization of the above granular HTSC composites and at finding a universal parameter characterizing the magnetoresistance hysteresis for various transport current densities.

## 2. EXPERIMENT

### 2.1. Preparation and Composition of Composite Samples

We prepared two-phase composites using the rapid sintering technique [35–40]. One of the components of the composite (HTSC) was prepared by the standard ceramic technology. After thorough grinding of the HTSC and the other (nonsuperconducting) ingredient (high-purity copper oxide in our case), the components are mixed and pressed into pellets that are placed in a preliminarily heated furnace. High-temperature annealing is carried out for a very short time to avoid chemical interaction between the components of the composite and the growth of crystallites, resulting in the formation of boundaries of a type of superconducting microbridges between HTSC grains. After this, the samples are placed in another furnace for saturating the HTSC with oxygen. Results similar to those presented below were obtained by us for various composites prepared using this technique. In this paper, we report on the results obtained for  $Y_{0.75}Lu_{0.25}Ba_2Cu_3O_7 + CuO$  composites. The temperature regime for these composites was as follows: 2-min holding at  $T = 910^\circ\text{C}$  followed by 3-h holding at  $T = 350^\circ\text{C}$ . According to X-ray diffrac-

tion data, the composites contain only two initial components ( $Y_{0.75}Lu_{0.25}Ba_2Cu_3O_7$  and CuO). According to scanning electron microscopy data, the mean size of HTSC grains in the composite amounts to about 1.5  $\mu\text{m}$ . Magnetic measurements of the composites show that all samples have the same superconducting transition temperature,  $T_c = 93.5$  K, which coincides with the superconducting transition temperature for the initial HTSC. We denote the composites in accordance with the volume concentration of CuO in these compounds as YBCO +  $V$ CuO, where  $V$  stands for the volume concentration of CuO in the composite (%), the concentration of the semiconductor (YBCO) being  $(100 - V)\%$ .

### 2.2. Experimental Techniques

Transport measurements were performed using the standard four-probe technique. The samples were sawed in the form of a parallelepiped  $1 \times 1 \times 8$  mm<sup>3</sup> in size. Since this size was the same for all samples, data on resistance  $R$  are given in ohms and on current  $I$  in milliamperes. In the measurements of magnetic field dependence  $I_c(H)$  of the critical current, the value of the external field was set and the  $IV$  characteristic was measured. The value of critical current  $I_c$  was determined using the standard criterion of 1  $\mu\text{V}/\text{cm}$  [41]. Then the external field was varied to its next value. Dependences  $R(H) = U(H)/I$  of the magnetoresistance were measured at a constant current  $I$ . The sample was cooled in zero external magnetic field. Magnetic field  $\mathbf{H}$  was applied at right angles to the direction of current. The magnetic-field scanning rate was approximately 300 Oe/min. We did not detect any effect of the field scanning rate on the  $R(H)$  dependence in the range 50–800 Oe/min. After an increase in the field from  $H = 0$  to a fixed value  $H_{\text{max}}$ , the external field was reduced to zero at the same rate. For recording the magnetic past history, the sample was heated to above  $T_c$  after a measuring cycle. We will denote an increasing external magnetic field ( $dH/dt > 0$ ) by  $H_\uparrow$  and a decreasing field ( $dH/dt < 0$ ) by  $H_\downarrow$ .

Magnetic measurements were performed on an automated vibrating-coil magnetometer with a superconducting solenoid [42]. The field scanning rate was the same as in the  $R(H)$  measurements.

### 2.3. Composites as a Network of Josephson Junctions

Figure 1 shows the  $R(T)$  dependences of the composites under investigation. The  $R(T)$  dependences are characterized by an abrupt resistance jump at  $T_c = 93.5$  K (which coincides with the superconducting transition temperature determined from magnetic measurements) followed by a smooth segment. The effect of transport current  $I$  and magnetic field on the  $R(T)$  dependences was investigated in detail in [37, 30]: an increase in  $I$  and application of the magnetic field do not affect the swing of the step, but expand the second (smooth) step on the  $R(T)$  dependences. For this reason,

<sup>1</sup> In its physical properties, this compound is identical to the classical  $YBa_2Cu_3O_7$  compound since Lu occupies yttrium positions in the 1–2–3 structure and does not change its superconducting properties, simultaneously facilitating the preparation process.

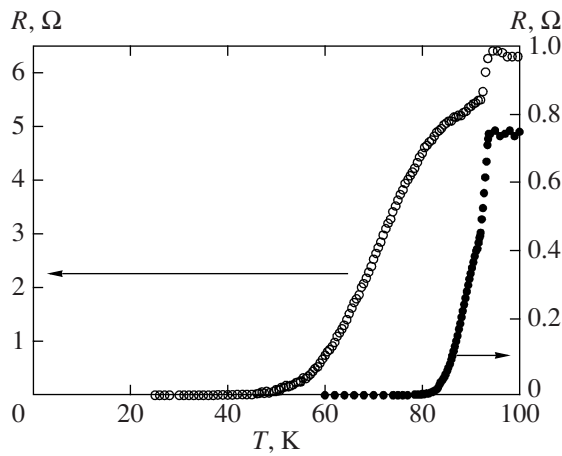


**Fig. 1.**  $R(T)$  dependences for the composites under investigation for a measuring current of 0.1 mA at  $T = 4.2$  K: YBCO + 15CuO,  $I_c = 80$  mA,  $j_c \approx 19$  A/cm<sup>2</sup> (●) and YBCO + 30CuO,  $I_c = 4.5$  mA,  $j_c \approx 0.5$  A/cm<sup>2</sup> (○).

the resistance jump is unambiguously interpreted as a transition of superconducting crystallites, while the second (smooth) step on the  $R(T)$  dependences is interpreted as a transition of the network of Josephson junctions. The values of the critical current density for the composites are given in Fig. 1. In the temperature range above  $T_c$ , the  $R(T)$  dependences of the composites are of the quasi-semiconducting type [37, 38], which also indicates that the transport current flows via HTSC grains as well as via the nonsuperconducting component.

### 3. RESULTS AND DISCUSSION

#### 3.1. Interrelation between Critical-Current and Magnetoresistance Hysteresis

Figure 2 shows the hysteresis loop in the field dependence of the critical current of the YBCO + 15CuO composite at  $T = 4.2$  K (the inset to the figure shows a segment of the  $I_c(H)$  curve in the range of weak fields). The direct branch of the  $I_c(H)$  dependence is characterized by a sharp decrease in the critical current in weak fields (tens of oersteds). The inverse branch  $I_c(H_{\downarrow})$  has a peak at a field  $H_{\text{ext}}$ . For  $H_{\text{max}} = 5$  kOe, at  $T = 4.2$  K, the value of  $H_{\text{ext}}$  amounts to approximately 1.1 kOe (see Fig. 2). The field  $H_{\text{ext}}$  in which the  $I_c$  peak is observed increases with  $H_{\text{max}}$ . The value of critical current  $I_c$  at the peak point decreases upon an increase in the strongest applied field  $H_{\text{max}}$ . The behavior of the  $I_c(H)$  dependence will be explained in Section 3.3; here, we will consider in greater detail the interrelation between  $I_c(H)$  and  $R(H)$ .

Figure 3 shows the  $R(H)$  dependences for the same YBCO + 15CuO sample, on which the  $I_c(H)$  dependence depicted in Fig. 2 was obtained for various values of transport current  $I$ . The strongest applied field  $H_{\text{max}} =$

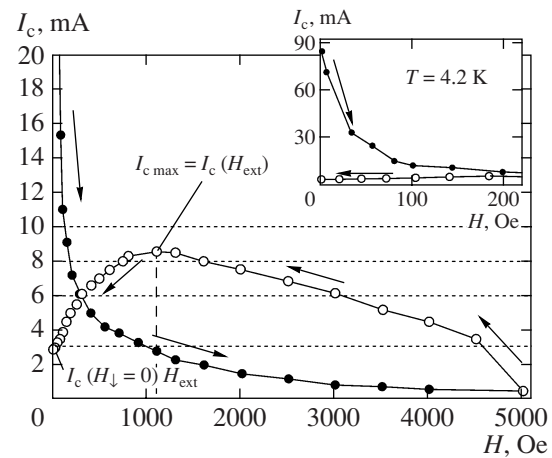


**Fig. 2.** Field dependence of critical current  $I_c(H)$  of the YBCO + 15CuO sample at  $T = 4.2$  K. The inset shows  $I_c(H)$  in the range of weak fields. Arrows indicate the directions of variation of external field  $\mathbf{H}$ . Horizontal dotted lines correspond to values of transport current  $I$  in the  $R(H)$  measurements presented in Fig. 3 and demonstrate the relation between  $I$  and  $I_c(H_{\uparrow})$ ,  $I_c(H_{\downarrow})$  for the investigation range of magnetic fields for  $I_c(H_{\downarrow} = H_{\text{ext}}) \approx 8.4$  mA and  $I_c(H_{\downarrow} = 0) \approx 3.0$  mA.

5 kOe is the same for  $R(H)$  dependences as well as for  $I_c(H)$  dependences. In all cases depicted in Fig. 3,  $I < I_c(H_{\uparrow} = 0)$ ; for this reason, a resistance of the  $R(H_{\uparrow})$  branch appears for threshold field  $H_{\text{thr}}$ , at which the critical current becomes equal to the measuring current,  $I_c(H_{\uparrow} = H_{\text{thr}}) = I$ , which can be seen from a comparison of the  $I_c(H)$  curves in Fig. 2 and  $R(H)$  curves in Fig. 3. The values of transport current used for measuring the  $R(H)$  dependences are too low to induce a magnetic field comparable to the external field. This is another factor favoring the use of composites since the field induced by transport current in polycrystals with “natural” intercrystallite boundaries makes a noticeable contribution [5].

Since resistance and transport current are inverse quantities [41], the  $I_c(H)$  branch with higher values of  $I_c$  corresponds to the  $R(H)$  branch with a lower resistance. If, however, the measuring current is smaller than the critical current depicted by the  $I_c(H_{\downarrow})$  curve in some regions of fields, the resistance described by the  $R(H_{\downarrow})$  curve will be again equal to zero in this range of the fields. The values of transport current  $I$  (3, 6, 8, and 10 mA) used for measuring the  $R(H)$  dependences (Fig. 3) are depicted in Fig. 2 by horizontal dashed lines. A comparison of the data presented in Figs. 2 and 3 shows the correlation between the  $I_c(H_{\downarrow})$  and  $R(H)$  dependences. For  $I = 3$  mA,  $I < I_c(H_{\downarrow} = H_{\text{ext}}) \approx 8.4$  mA, a wide field interval exists in the  $R(H)$  dependence ( $H_{\downarrow} \leq 4.6$  kOe), on which  $R = 0$  (see Fig. 3a). And since  $I_c(H_{\downarrow} = 0) \approx 3$  mA =  $I$  (see Fig. 2), the residual resistance of the sample is equal to zero ( $R(H_{\downarrow} = 0) \approx 0$ ) for the given transport current  $I = 3$  mA. Upon an increase in transport current ( $I > I_c(H_{\downarrow} = 0) \approx 3$  mA),

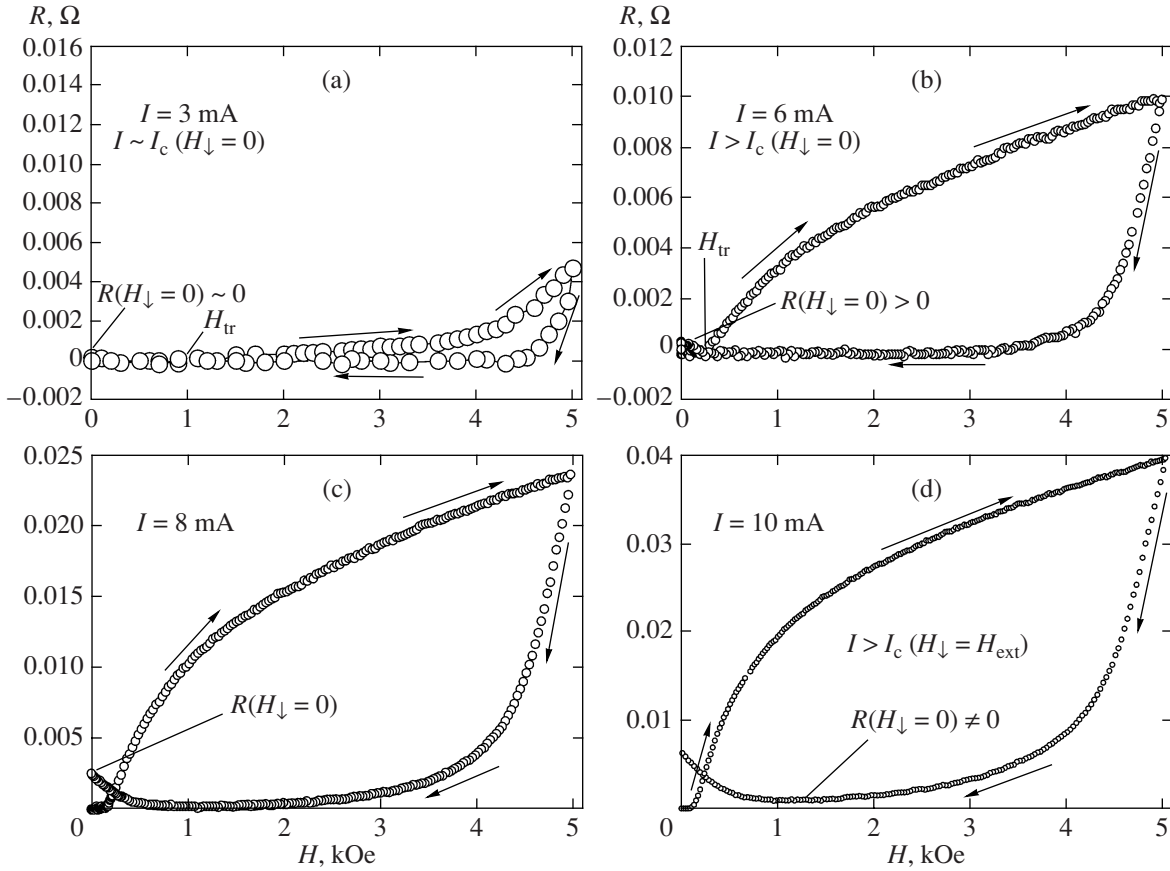


**Fig. 3.**  $R(H)$  dependences for the YBCO + 15CuO sample at various relations between transport current  $I$  (3, 6, 8, 10 mA) and critical current  $I_c(H_\perp = H_{\text{ext}}) \approx 8.4$  mA and  $I_c(H_\perp = 0) \approx 3.0$  mA (see Fig. 2). Arrows indicate the direction of variation of external field  $\mathbf{H}$ . Measuring current  $I$ , field  $H_{\text{thr}}$  at which a nonzero voltage drop appears, and residual resistance  $R(H_\perp = 0)$  after the action of magnetic field  $H_{\text{max}} = 5$  kOe are indicated in the figures.

a nonzero residual resistance  $R_{\text{res}}$  appears, which increases with current (see Figs. 3b–3d) since the  $IV$  characteristics are nonlinear. In addition, the range of fields  $H_\perp$  in which  $R = 0$  decreases upon an increase in transport current. This can be seen from Figs. 3b and 3c; for  $I = 6$  mA, zero resistance is observed in the field range  $0.4 \text{ kOe} \leq H_\perp \leq 3.0 \text{ kOe}$  (see Fig. 3b). For  $I = 8$  mA, the region with  $R = 0$  becomes still narrower ( $0.8 \text{ kOe} \leq H_\perp \leq 1.5 \text{ kOe}$ ; see Fig. 3c), while for current  $I = 10$  mA, which is larger than  $I_c(H_\perp = H_{\text{ext}}) \approx 8.4$  mA, the  $R(H_\perp)$  dependence does not attain zero and acquires a minimum (see Fig. 3d). The field in which the minimum is observed on the  $R(H_\perp)$  dependence coincides with field  $H_{\text{ext}}$ , at which the  $I_c(H)$  dependence has a maximum (see Fig. 2).

No experimental results showing the evolution of  $R(H)$  (the segment with zero resistance on the  $H_\perp$  branch or the emergence of residual resistance and a minimum) have been reported so far for granular HTSCs in which transport current increases from a value  $I$  lower than  $I_c(H_\perp = H_{\text{ext}})$  to a value exceeding the peak on the  $I_c(H_\perp)$  dependence. Here, we demonstrate experimentally that residual resistance appears on the  $R(H)$  dependence for a transport current  $I$  higher than

the critical current after the action of a magnetic field (i.e., for  $I > I_c(H_\perp = 0)$ ), while the segment with zero resistance or a minimum on the backward branch of  $R(H)$  is determined by the relation between the measuring and critical currents at the peak point on the  $I_c(H)$  dependence.

### 3.2. Model for Granular HTSCs

We can approximately treat a granular HTSC as a two-level superconducting system [15]: HTSC crystallites with strong superconductivity and intercrystallite boundaries forming weak bonds of the Josephson type. It is known that the lower critical field  $H_{c1J}$  of a Josephson medium for granular HTSCs at high temperatures ( $\sim 77$  K) is weaker than the field of the Earth [18, 33], while the lower critical field  $H_{c1g}$  for Y–Ba–Cu–O grains is on the order of tens of oersteds [18, 20, 22, 29]. At helium temperatures, these parameters increase, but only by a factor of several units. For example, the value of  $H_{c1J}$  for Y–Ba–Cu–O grains is on the order of 100–200 Oe at  $T = 4.2$  K [43]. Critical current density  $j_{cJ}$  of the network of Josephson junctions ( $j_{cJ} \sim 10^3$  A/cm<sup>2</sup> for

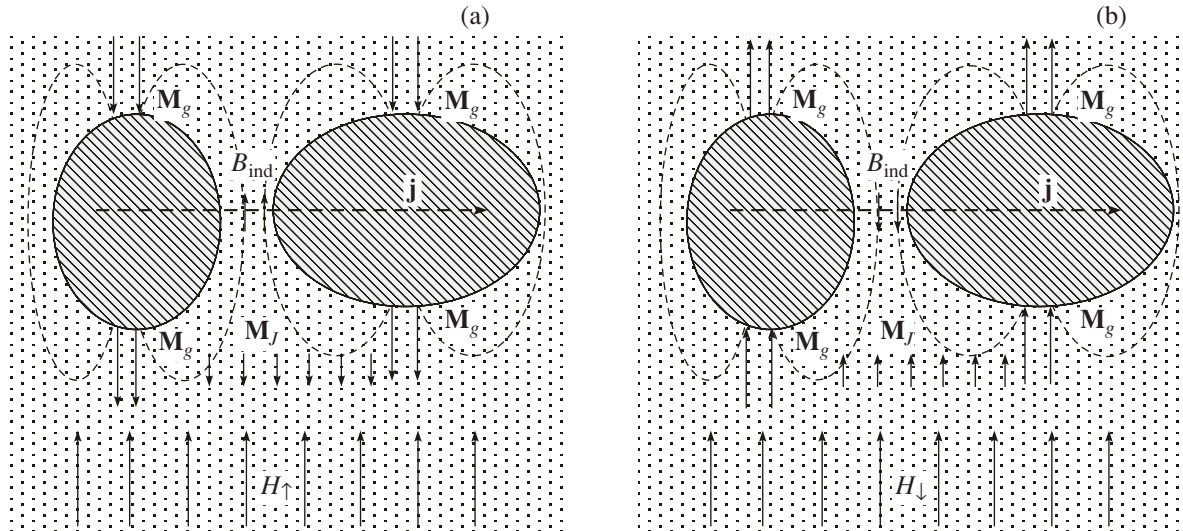


**Fig. 4.** Schematic representation of a granular HTSC in an external field  $\mathbf{H}$ . Superconducting grains are hatched, intergranular medium is indicated by points. The direction of transport current density  $\mathbf{j}$ ,  $\mathbf{j} \perp \mathbf{H}$ , is indicated; (a) external field increases ( $\mathbf{H} = H_{\uparrow}$ ) and (b) decreases ( $\mathbf{H} = H_{\downarrow}$ ) after the application of a certain field  $H_{\text{max}}$ ;  $\mathbf{M}_g$  is the magnetic moment of HTSC grains; the external field  $H_{\downarrow}$  in (b) differs substantially from  $H_{\text{max}}$  and magnetization assumes positive values (see the  $M(H_{\downarrow})$  curve for the sample under investigation in Fig. 5).  $\mathbf{M}_J$  is the magnetic moment of the Josephson medium, which is much smaller in magnitude than  $\mathbf{M}_g$ . Dashed curves are the lines of the magnetic field induced by the magnetic response of HTSC grains.

HTSC polycrystals and  $j_{cJ} \sim 10^{-1} - 10^2$  A/cm<sup>2</sup> for composites at helium temperature) is much lower than the intergrain critical current density  $j_{cg}$  ( $j_{cg} \sim 10^5 - 10^7$  A/cm<sup>2</sup>),  $j_{cJ} \ll j_{cg}$ . In addition, inequalities  $H \ll H_{c2g}$  ( $H_{c2g}$  is the upper critical field for HTSC grains) and  $j \ll j_{cg}$  hold in almost all experiments in the low-temperature region. Consequently, if a granular HTSC possesses a nonzero resistance, the entire dissipation in an external magnetic field and in zero field occurs only in the Josephson medium. Fields stronger than  $H_{c1J}$  penetrate the system of intercrystallite boundaries in the form of hypervortices or Josephson vortices whose size decreases with increasing field [18, 33]. In view of the strong magnetic field dependence of the critical current (and, hence, resistance) of Josephson junctions [41], as well as an enormously large number of intercrystallite boundaries (on the order of  $10^3$  per millimeter) in a polycrystal, these objects demonstrate a high sensitivity to an external field.

Let us first simplify the above-mentioned two-level system, assuming that pinning in Josephson barriers (i.e., intergranular boundaries) is negligibly weak and the magnetic flux is trapped only in superconducting grains. We also assume that the contribution of grain boundaries to the diamagnetic response of the sample is also negligibly small. In this case, for  $H > H_{c1J}$ , a local field  $\mathbf{B}_{\text{local}}$  is acting on each point of the Josephson medium, which is equal to the vector sum of external field  $\mathbf{H}$  and field  $\mathbf{B}_{\text{ind}}$  induced by the diamagnetic response of the grains surrounding a given point:

$$\mathbf{B}_{\text{local}} = \mathbf{H} + 4\pi\mathbf{M}k, \quad \mathbf{B}_{\text{ind}} = 4\pi\mathbf{M}k, \quad (1)$$

where  $k$  is a coefficient depending on the position and shape of the grains surrounding a given point and  $\mathbf{M}$  is the magnetization of HTSC grains. Figure 4 shows schematically the lines of magnetic induction  $\mathbf{B}_{\text{ind}}$  in the Josephson medium, which emerge from the diamagnetic response of HTSC grains. Let us consider the direction of  $\mathbf{B}_{\text{ind}}$  at the boundary between two HTSC grains, through which current carriers are tunneling ( $\mathbf{j} \perp \mathbf{H}$ ). In an increasing external field (Fig. 4a), the lines of magnetic induction  $\mathbf{B}_{\text{ind}}$  in most of junctions carrying transport current are predominantly directed in the same direction as external field  $\mathbf{H}$ . Consequently, local fields in this region of the boundaries between grains are stronger than the external field. If the external field decreases ( $H = H_{\downarrow}$ ; Fig. 4b) and  $H_{\downarrow}$  differs substantially from  $H_{\text{max}}$ , the magnetization of grains becomes positive (Fig. 5; this follows from classical analysis of pinning of Abrikosov vortices). In this case, magnetic induction lines  $\mathbf{B}_{\text{ind}}$  in the region of HTSC grain boundaries considered here are directed oppositely to the external field. We can speak of effective field  $B_{\text{eff}}$ , in which the Josephson medium is located if we average the values of modulus  $|\mathbf{B}_{\text{local}}|$  over all grain boundaries through which charge carriers are tunneling:

$$B_{\text{eff}} = \langle |\mathbf{B}_{\text{local}}| \rangle = H - 4\pi M(H)\alpha(H). \quad (2)$$

Quantity  $\alpha$  appears as a result of averaging of coefficient  $k$  in formulas (1) over all Josephson junctions in the sample. The  $M(H)$  dependence for grains is determined by Meissner currents as well as by Abrikosov vortices. Consequently,  $\alpha$  is a function of external field  $H$ .

The expression for the effective field becomes more complicated if we take pinning in the Josephson medium and its magnetization  $M_j$ . The latter is the response of the Josephson medium to the superposition of external field  $H$  and field  $\mathbf{B}_{\text{ind}}$  induced by the grains. In the general case,  $\mathbf{M}_j$  is directed in the same way as the grain magnetization  $\mathbf{M}_g$ . In the region of grain boundaries considered here,  $\mathbf{M}_j$  makes a contribution to  $\mathbf{B}_{\text{local}}$  opposite to that of  $\mathbf{B}_{\text{ind}}$  (see Fig. 4). An analogous result was obtained in [34], where the magnetization curves for granular HTSC were considered. Analogously to relation (2), we can write

$$B_{\text{eff}} = H - 4\pi(M_g(H)\alpha(H) - M_j(H, j)). \quad (3)$$

In accordance with the concepts concerning the behavior of vortices in a superconductor in the case when transport current flows in the presence of a magnetic field, a current stronger than the critical current radically changes the profile of the coordinate function of the pinning potential [44–46]. As a result of action of the Lorentz force, vortices are detached from the pinning centers. For this reason,  $M_j$  is a function of transport current. Consequently, if pinning in the Josephson medium is significant, we can expect that transport current affects the effective field  $B_{\text{eff}}$  in the Josephson medium.

### 3.3. Effective Field in the Josephson Medium and Hysteresis of $I_c(H)$ and $R(H)$

Expressions (2) and (3) explain the hysteresis in the  $I_c(H)$  and  $R(H)$  dependences in terms of the known hysteresis of  $M(H)$ . The  $M(H)$  dependences measured in a YBCO + 30CuO sample are shown in Fig. 5. Since  $M(H_{\downarrow}) > M(H_{\uparrow})$  for  $H_{\uparrow} = H_{\downarrow}$ , we have  $B_{\text{eff}}(H_{\uparrow}) < B_{\text{eff}}(H_{\downarrow})$  in accordance with relation (2). As a result, the critical current in a decreasing field will be larger than in an increasing field and, hence,  $R(H_{\downarrow}) < R(H_{\uparrow})$ . Upon a further decrease in the external field, the external field at a certain instant is compensated to the highest extent by field  $\mathbf{B}_{\text{ind}}$  induced by grains and, hence, effective field  $B_{\text{eff}}$  is the weakest. Precisely at this point, at  $H = H_{\text{ext}}$ , a peak is observed in the critical current in the  $I_c(H_{\downarrow})$  dependence and a minimum in the  $R(H_{\downarrow})$  dependence. Upon a further decrease in  $H$  below  $H_{\text{ext}}$ , the field induced by the frozen flux will prevail over the external field, the value of  $B_{\text{eff}}$  will increase and, hence, the critical current will decrease and the resistance will increase, which is observed in experiments (see Figs. 2 and 3b–3d). In zero external field  $H_{\downarrow} = 0$ , the sample possesses a positive magnetic moment (see Fig. 5) and induced field  $B_{\text{ind}}$  remains in the intergranular medium. For this reason, the sample possesses a nonzero residual resistance.

Figure 6 shows hysteretic dependences  $R(H)$  for the YBCO + 30CuO sample for various values of transport current (2–10 mA) and for various fixed values of

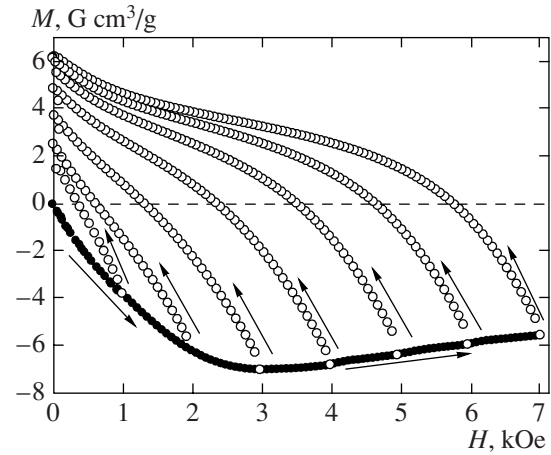


**Fig. 5.** Dependences of the magnetization of the YBCO + 30CuO sample on external field  $\mathbf{H}$  at  $T = 4.2$  K. Arrows indicate the direction of variation of  $\mathbf{H}$ . Each measurement for a new value of  $H_{\text{max}}$  is performed after recording magnetic past history. The  $R(H_{\uparrow})$  dependences (in increasing field) are shown by dark circles, while the  $R(H_{\downarrow})$  dependences (in decreasing field) are shown by light circles.

$H_{\text{max}} = 1, 2, 3, \dots, 7$  kOe. It can be clearly seen from Fig. 6 that both the residual resistance  $R(H_{\downarrow} = 0)$  and the value of field  $H_{\text{ext}}$  (in which a minimum is observed on the  $R(H_{\downarrow})$  dependence) increase upon an increase in the maximum applied field  $H_{\text{max}}$ . Such a behavior takes place due to the fact that a larger magnetic flux is trapped in superconducting grains and the value of  $B_{\text{eff}}$  increases upon an increase in  $H_{\text{max}}$ . As a result, the most complete compensation of the external and induced fields occurs at a higher value of  $H_{\downarrow} = H_{\text{ext}}$  and a stronger effective field is induced in the Josephson medium at point  $H_{\downarrow} = 0$  and, as a result, the value of  $R(H_{\downarrow} = 0)$  increases with  $H_{\text{max}}$ .

### 3.4. Effect of Transport Current on Hysteretic $R(H)$ Dependences

The low current density for the YBCO + 30CuO composite makes it possible to study the  $R(H)$  dependences at  $T = 4.2$  K in the case when the value of transport current is higher than not only the critical current at the point of maximum  $j(H_{\downarrow} = H_{\text{ext}})$ , but also the critical current in zero field ( $j > j_c(H_{\uparrow} = 0)$ ). Hysteretic  $R(H)$  dependences for the YBCO + 30CuO sample shown in Fig. 6 were measured for values of transport current ( $I = 2$ –10 mA) both smaller than the critical current in zero field ( $I_c(T = 4.2$  K,  $H = 0) \approx 4.5$  mA) and larger than this value. We will concentrate our attention on the effect of current on the field width of the hysteresis loop  $R(H)$ .

The equality of resistance values in fields  $H_{\uparrow}$  and  $H_{\downarrow}$ ,  $R(H_{\uparrow}) = R(H_{\downarrow})$ , indicates the equality of effective fields at these points:  $B_{\text{eff}}(H_{\uparrow}) = B_{\text{eff}}(H_{\downarrow})$ . In the case when pinning in the Josephson medium and the contri-

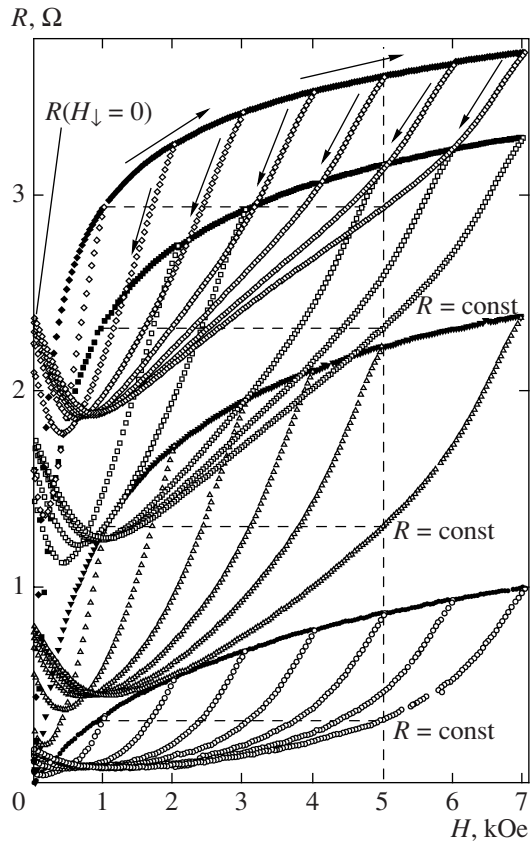


**Fig. 6.**  $R(H)$  dependences for the YBCO + 30CuO sample at various values of transport current  $I$  (2, 4, 7, and 10 mA from bottom to top) and various values of the maximal applied field  $H_{\max} = 1, 2, 3, \dots, 7$  kOe at  $T = 4.2$  K. Arrows indicate the direction of variation of external field  $\mathbf{H}$ . The  $R(H_{\uparrow})$  dependences (in increasing field) are shown by dark circles, while the  $R(H_{\downarrow})$  dependences (in decreasing field) are shown by light circles. Each measurement for a new value of  $H_{\max}$  is performed after recording magnetic past history. Dashed lines illustrate the determination of the field width of the hysteresis loop  $\Delta H_{R=\text{const}} = H_{\downarrow} - H_{\uparrow}$ .

bution to magnetization from this medium are small, we obtain from relation (2)

$$H_{\uparrow} - 4\pi M(H_{\uparrow})\alpha(H_{\uparrow}) = H_{\downarrow} - 4\pi M(H_{\downarrow})\alpha(H_{\downarrow}). \quad (4)$$

Consequently, the width  $\Delta H = H_{\downarrow} - H_{\uparrow}$  of the magnetoresistance hysteresis loop for  $R = \text{const}$  is given by

$$\begin{aligned} \Delta H_{R=\text{const}} &= H_{\downarrow} - H_{\uparrow} \\ &= 4\pi(M(H_{\downarrow})\alpha(H_{\downarrow}) - M(H_{\uparrow})\alpha(H_{\uparrow})). \end{aligned} \quad (5)$$

It can be seen that parameter  $\Delta H_{R=\text{const}}$  depends only on magnetization and is independent of transport current. It was noted in Section 3.2 that the values of  $\alpha(H_{\uparrow})$  and  $\alpha(H_{\downarrow})$  are different due to pinning and, as a consequence, different magnetic states of grains on the direct and reverse branches of the  $M(H)$  dependence. Analysis of our experimental results on the  $R(H)$  and  $M(H)$

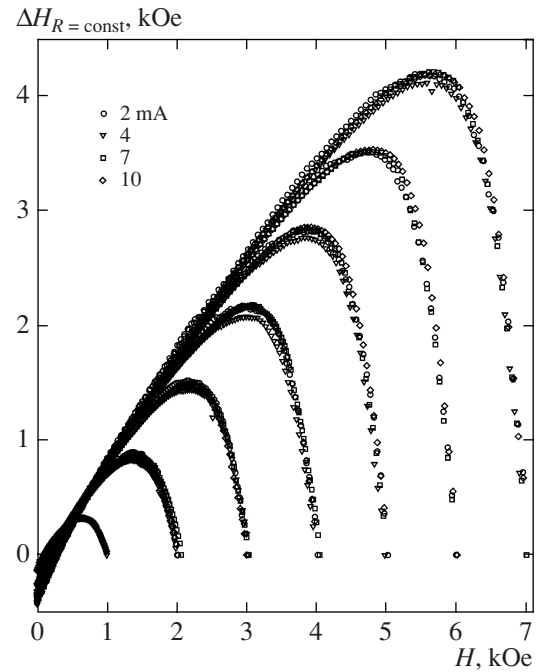


**Fig. 7.** Magnetoresistance hysteresis loop width  $\Delta H_{R=\text{const}} = H_{\downarrow} - H_{\uparrow}$  for  $R = \text{const}$  (transport current ranges from 2 to 10 mA) as a function of the values of  $H_{\downarrow}$  for various values of  $R(H)$  of the YBCO + 30CuO sample depicted in Fig. 6.

dependences obtained for the same sample confirm this statement.

In the case when pinning of vortices in the Josephson medium can make a noticeable contribution to local field (1), we obtain from Eq. (3)

$$\begin{aligned} \Delta H_{R=\text{const}} &= H_{\downarrow} - H_{\uparrow} = 4\pi(M_g(H_{\downarrow})\alpha(H_{\downarrow}) \\ &- M_J(H_{\downarrow}, j)) - 4\pi(M(H_{\uparrow})\alpha(H_{\uparrow}) - M_J(H_{\uparrow}, j)). \end{aligned} \quad (6)$$

In this case, the width of the magnetoresistance hysteresis loop must depend on transport current in view of the  $M_J(H, j)$  dependences.

Analyzing our experimental results presented in Fig. 6, as well as the data obtained for other composite samples, we discovered that the magnetoresistance hysteresis loop width is indeed independent of transport current (naturally, in the case when the value of transport current  $I$  is higher than  $I_c(H_{\downarrow} = H_{\text{ext}})$  and when  $R(H_{\downarrow})$  does not vanish; see Section 3.1). Figure 7 illustrates this statement. The figure shows  $\Delta H_{R=\text{const}} = (H_{\downarrow} - H_{\uparrow})$  as a function of  $H_{\downarrow}$  (in other words, the length of the segment between the points of intersection of the line  $R = \text{const}$  with the  $R(H_{\uparrow})$  and  $R(H_{\downarrow})$  curves for the data presented in Fig. 6 as a function of field  $H_{\downarrow}$ ). The data on  $\Delta H_{R=\text{const}}$  for  $R(H)$  measurements at different currents coincide to within the experimental error; i.e., the difference  $\Delta H_{R=\text{const}} = H_{\downarrow} - H_{\uparrow}$  remains unchanged in spite of the fact that the shape of the  $R(H_{\uparrow})$  and  $R(H_{\downarrow})$  curves strongly changes upon an increase in current (see Fig. 6). The value of  $\Delta H_{R=\text{const}}$  is determined only

by the maximal applied field  $H_{\max}$  (i.e., by the flux trapped in grains or by intergranular pinning). Proceeding from the above considerations, we believe that the independence of the hysteresis loop width of transport current can be interpreted unambiguously as the fact that the magnetoresistance hysteresis for objects studied here is controlled only by the flux trapped in HTSC grains.

### 3.5. Magnetic Past History and Specific $R(H)$ Hysteresis Loops

Let us consider in greater detail the effect of the flux trapped by grains after the action of the field on the  $R(H)$  dependences. Figure 8a shows the hysteretic dependences of the resistance of an S + 30CuO sample at  $T = 4.2$  K, which were measured after zero-field cooling as well as after the application and removal of field  $H_{\max} = 2$  kOe. To distinguish between the  $R(H)$  dependences with magnetic past history and without it, we denote the field dependences of resistance after the action of field  $H_{\max}$  by  $R_{\text{trapped}}(H)$  (see also the caption to Fig. 8). The segment of the  $R_{\text{trapped}}(H_{\uparrow})$  dependence with a negative magnetoresistance in the region of low field is worth noting (see Fig. 8a). Passing through a minimum, the  $R_{\text{trapped}}(H_{\uparrow})$  dependence increases and coincides with the  $R(H_{\uparrow})$  dependence in a field of 2 kOe (i.e., in the maximum field  $H_{\max}$  applied to the sample earlier). The  $R_{\text{trapped}}(H_{\downarrow})$  dependence coincides with the  $R(H_{\downarrow})$  dependence, including the value for  $H_{\downarrow} = 0$ . Upon a further variation of the field from 0 to  $H_{\max} = 2$  kOe, the  $R_{\text{trapped}}(H)$  dependences repeat themselves. If we increase the field again upon a decrease of the external field to a certain nonzero value  $H_{\downarrow}$ , the  $R_{\text{trapped}}(H_{\uparrow})$  and  $R(H_{\uparrow})$  dependences again coincide at point  $H_{\uparrow} = H_{\max}$ . This can be seen in Fig. 8 where a specific hysteresis loop  $R_{\text{trapped}}(H)$  is depicted in the field range  $1 \text{ kOe} \leq H \leq 2 \text{ kOe}$ . If we increase the external field at point  $H = H_{\max} = 2$  kOe, the  $R_{\text{trapped}}(H_{\uparrow})$  dependence on segment  $H \geq H_{\max}$  behaves in the same way as after zero-field cooling.

Figure 8b shows the  $M(H)$  dependences measured on the same sample in the same sequence as the  $R(H)$  dependence was measured in Fig. 8a. It can be seen that the grain magnetization is positive at point  $H_{\downarrow} = 0$ . After the application or removal of the magnetic field, the trapped magnetic flux remaining in the grains induces a field in the intergranular medium. If we increase the external field in positive direction,  $\mathbf{B}_{\text{ind}}$  will be directed oppositely to  $\mathbf{H}$ , and the effective field defined by expression (2) will decrease. This explains the existence of the segment with a negative magnetoresistance in the  $R_{\text{trapped}}(H_{\uparrow})$  dependence. At the point of maximum compensation of the external field and the field induced by grains, the  $R_{\text{trapped}}(H_{\uparrow})$  dependence has a minimum (see Fig. 8a). With increasing external field, magnetization decreases and becomes negative (see Fig. 8b), and  $\mathbf{B}_{\text{ind}}$  will coincide in direction with the external field. It follows from the results of our experi-

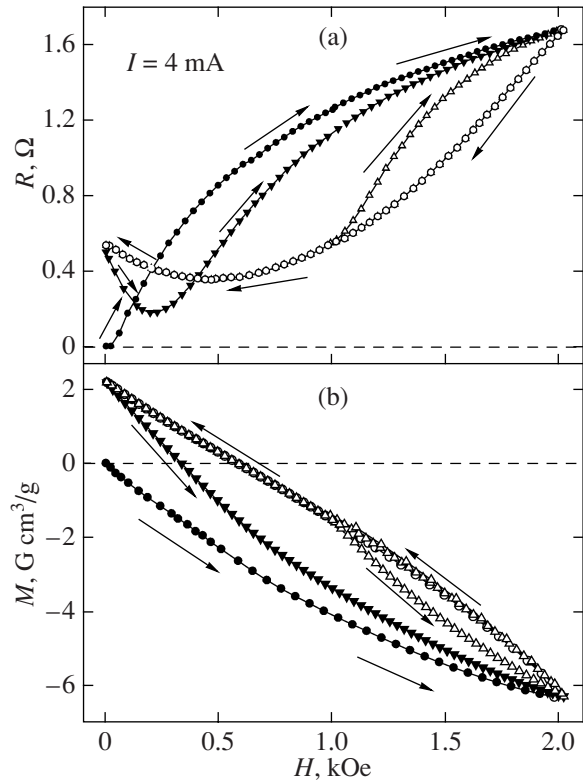


**Fig. 8.** Effect of magnetic past history on the (a)  $R(H)$  and (b)  $M(H)$  dependences for a YBCO + 30CuO sample at  $T = 4.2$  K. Arrows indicate the direction of variation of external field  $\mathbf{H}$ . The  $R(H_{\uparrow})$  and  $M(H_{\uparrow})$  dependences (in increasing field) are shown by dark symbols, while the  $R(H_{\downarrow})$  and  $M(H_{\downarrow})$  dependences (in decreasing field) are shown by light symbols. Dark circles correspond to measurements after zero-field cooling, while dark triangles correspond to measurements after the application of field  $H_{\max} = 2$  kOe.

ments that the field in which the minimum is observed on the  $R_{\text{trapped}}(H_{\uparrow})$  dependence is independent of transport current and is determined only by the value of  $H_{\max}$ . This additionally confirms the conclusion drawn in Section 3.4 concerning the fact that the hysteresis on the  $R(H)$  dependence for the samples under investigation is caused exclusively by magnetic flux trapping in superconducting grains. At point  $H = H_{\max}$ , sample magnetization  $M_{\text{trapped}}$  coincides with the value of  $M$  measured during zero-field cooling (see Fig. 8b); i.e., at point  $H_{\uparrow} = H_{\max}$ , the sample passes to the same magnetic state as during the first application of the magnetic field. Consequently, in the given field  $H = H_{\max}$ , the effective field in the intergranular medium is the same as in measurements after zero-field cooling. This explains the equality of values  $R_{\text{trapped}}(H_{\uparrow} = H_{\max})$  and  $R(H_{\uparrow} = H_{\max})$  and the coincidence of the  $R_{\text{trapped}}(H_{\downarrow})$  and  $R(H_{\downarrow})$  dependences (see also dependences  $M_{\text{trapped}}(H_{\downarrow})$  and  $M(H_{\downarrow})$  in Fig. 8b).

If we apply a negative external field at point  $H_{\downarrow} = 0$  after the action with the field up to  $H_{\max}$ , it will make a contribution to  $B_{\text{eff}}$  of the same sign as that from the

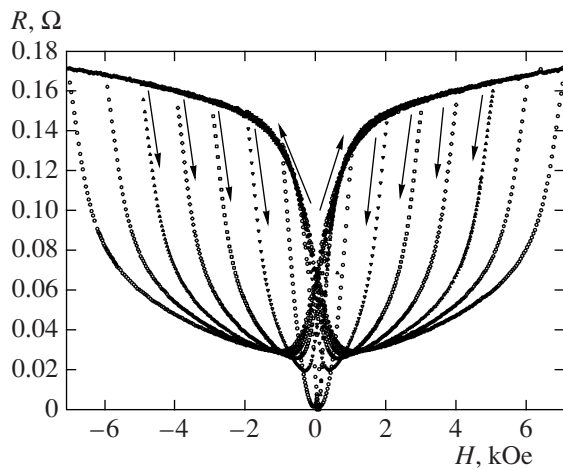


**Fig. 9.** Hysteretic  $R(H)$  dependences for the YBCO + 15CuO sample at  $T = 5$  K (measuring current is 12 mA) upon field variation from  $H = 0$  to  $H_{\max}$ , and then from  $H = -H_{\max}$  to  $H = 0$ . Arrows indicate the direction of variation of external field  $\mathbf{H}$ .

field induced by grains. As a result, the magnetoresistance will be positive in the region  $H_{\uparrow} < 0$ . On the reverse branch of the external magnetic field from  $-H_{\max}$ , the induced field is again opposite to the external field and  $B_{\text{ind}}(H_{\uparrow}) < B_{\text{ind}}(H_{\downarrow})$ . Thus, when field  $\mathbf{H}$  is applied in the negative direction, the pattern of mutual arrangement of vectors  $\mathbf{H}$  and  $\mathbf{B}_{\text{ind}}$  depicted in Fig. 4 will be repeated (directions of  $\mathbf{H}$  and  $\mathbf{B}_{\text{ind}}$  will be reversed). Since dissipation is independent of the polarity of the field, the  $R(H)$  dependence obtained upon field cycling from  $-H_{\max}$  to  $H_{\max}$  will be symmetric relative to the straight line  $H = 0$  and has the shape of a butterfly (Fig. 9).

Thus, the magnetoresistance curves plotted after the action of an external field, as well as specific  $R(H)$  hysteresis loops, are determined by the magnetic state of superconducting grains in the sample.

### CONCLUSIONS

We studied experimentally the hysteretic dependences of the magnetoresistance of two-phase composites  $Y_{0.75}Lu_{0.25}Ba_2Cu_3O_7 + CuO$ . These objects can be treated as model granular HTSCs in which Josephson bonds between HTSC crystallites are artificially weakened.

It has been shown experimentally that the residual resistance, the segment with zero resistance, and the minimum on the inverse branch on the  $R(H)$  dependence are determined by the relation between the transport current and the critical current at the point of the maximum on the  $I_c(H_{\downarrow})$  curve.

The  $I_c(H)$  and  $R(H)$  hysteretic dependences, as well as negative magnetoresistance, are explained using the model of a granular HTSC with magnetic flux trapping

in grains. The intergranular medium is in the effective field, which is a superposition of external field  $\mathbf{H}$ , the field of Meissner currents, and the field induced by the trapped magnetic flux. Grain boundaries (i.e., Josephson junctions) form a sensitive “resistive sensor” responding to this effective field.

It is shown that the hysteretic  $R(H)$  dependences are characterized by a universal parameter (field width  $\Delta H_{R=\text{const}} = H_{\downarrow} - H_{\uparrow}$  of the hysteresis loop), which is independent on transport current density and is determined only by the magnetic flux trapped in superconducting grains. The effect of magnetic flux trapping in the Josephson medium is insignificant for the hysteresis in the transport properties of the investigated objects.

### ACKNOWLEDGMENTS

The authors are grateful to A.D. Balaev, S.V. Komogortsev, A.V. Mitin, L.P. Ichkitidze, and N.D. Kuz'michev for fruitful discussions.

This study was supported by the program “Quantum Macrophysics” of the Russian Academy of Sciences; complex integration project no. 3.4 of the Siberian Branch, Russian Academy of Sciences; Lavret'ev competition of projects by young scientists, Siberian Branch, Russian Academy of Sciences (project no. 52); grant no. MK-7414.2006.02 from the President of the Russian Federation in support of young scientists; and the Foundation for Promoting National Science.

### REFERENCES

1. H. Nojima, S. Tsuchimoto, and S. Kataoka, *Jpn. J. Appl. Phys.* **27**, 746 (1988).
2. Y. J. Quian, Z. M. Yang, K. Y. Chen, et al., *Phys. Rev. B* **39**, 4701 (1989).
3. K. Y. Chen and Y. J. Quian, *Physica C (Amsterdam)* **159**, 131 (1989).
4. G. J. Russel, D. N. Matthews, K. N. R. Taylor, and B. Perczuk, *Mod. Phys. Lett. B* **3**, 437 (1989).
5. M. E. McHenry, P. P. Maley, and J. O. Willis, *Phys. Rev. B* **40**, 2666 (1989).
6. B. A. Aronzon, Yu. V. Gershanov, E. Z. Meilikhov, and V. G. Shapiro, *Sverkhprovodimost: Fiz. Khim. Tekh.* **2**, 83 (1989).
7. N. V. Afanas'ev, Yu. E. Grigorashvili, and Yu. A. Chaplygin, *Sverkhprovodimost: Fiz. Khim. Tekh.* **3**, 2343 (1990).
8. Yu. S. Karimov and A. D. Kikin, *Sverkhprovodimost: Fiz. Khim. Tekh.* **3**, 631 (1990).
9. Ya. V. Kopelevich, V. V. Lemanov, and V. V. Makarov, *Fiz. Tverd. Tela (Leningrad)* **32**, 3613 (1990) [*Sov. Phys. Solid State* **32**, 2095 (1990)].
10. M. A. Vasyutin, A. I. Golovashkin, N. D. Kuz'michev, et al., Preprint No. 85, FIAN SSSR (Physical Inst., USSR Academy of Sciences, Moscow, 1990).
11. D. N. Matthews, G. J. Russel, and K. N. R. Taylor, *Physica C (Amsterdam)* **171**, 301 (1990).

12. E. Altshuler, S. Garcia, and J. Barroso, *Physica C* (Amsterdam) **177**, 61 (1991).
13. A. I. Ponomarev, K. R. Krylov, M. V. Medvedev, et al., *Sverkhprovodimost: Fiz. Khim. Tekh.* **4**, 2149 (1991).
14. M. Celasco, A. Masoero, P. Mazzetti, and A. Stepanescu, *Phys. Rev. B* **44**, 5366 (1991).
15. L. Ji, M. S. Rzchowski, N. Anand, and M. Tinkham, *Phys. Rev. B* **47**, 470 (1993).
16. M. Prester and Z. Mahornic, *Phys. Rev. B* **47**, 2801 (1993).
17. A. V. Mitin, *Sverkhprovodimost: Fiz. Khim. Tekh.* **7**, 62 (1994).
18. N. D. Kuz'michev, *Pis'ma Zh. Éksp. Teor. Fiz.* **74**, 291 (2001) [*JETP Lett.* **74**, 262 (2001)].
19. P. Mune, E. Govea-Alcaide, and R. F. Jardim, *Physica C* (Amsterdam) **354**, 275 (2001).
20. D. Daghero, P. Mazzetti, A. Stepanescu, et al., *Phys. Rev. B* **66**, 11478 (2002).
21. C. A. M. dos Santos, M. S. da Luz, B. Ferreira, and A. J. S. Machado, *Physica C* (Amsterdam) **391**, 345 (2003).
22. P. Mune, F. C. Fonesca, R. Muccillo, and R. F. Jardim, *Physica C* (Amsterdam) **390**, 363 (2003).
23. L. Burlachkov, E. Mogilko, Y. Schlessinger, et al., *Phys. Rev. B* **67**, 104509 (2003).
24. O. V. Gerashchenko, *Supercond. Sci. Technol.* **16**, 690 (2003).
25. I. Felner, E. Galstyan, B. Lorenz, et al., *Phys. Rev. B* **67**, 134506 (2003).
26. A. Sukhanov and V. Omel'chenko, *Fiz. Nizk. Temp.* **29**, 396 (2003) [*Low Temp. Phys.* **29**, 297 (2003)].
27. A. Sukhanov and V. Omel'chenko, *Fiz. Nizk. Temp.* **30**, 604 (2004).
28. V. V. Derevyanko, T. V. Sukhareva, and V. A. Finkel', *Fiz. Tverd. Tela* (St. Petersburg) **46**, 1740 (2004) [*Phys. Solid State* **46**, 1798 (2004)].
29. V. V. Derevyanko, T. V. Sukhareva, and V. A. Finkel', *Fiz. Tverd. Tela* (St. Petersburg) **48**, 1374 (2006) [*Phys. Solid State* **48**, 1455 (2006)].
30. D. A. Balaev, S. I. Popkov, K. A. Shaikhutdinov, and M. I. Petrov, *Fiz. Tverd. Tela* (St. Petersburg) **48**, 588 (2006) [*Phys. Solid State* **48**, 826 (2006)].
31. L. P. Ichkitidze, *Physica C* (Amsterdam) **435**, 136 (2006).
32. D. A. Balaev, A. G. Prus, K. A. Shaikhutdinov, and M. I. Petrov, *Pis'ma Zh. Tekh. Fiz.* **32** (8), 67 (2006) [*Tech. Phys. Lett.* **32**, 680 (2006)].
33. É. B. Sonin, *Pis'ma Zh. Éksp. Teor. Fiz.* **47**, 415 (1988) [*JETP Lett.* **47**, 496 (1988)].
34. M. Mahel' and J. Pivarc, *Physica C* (Amsterdam) **308**, 147 (1998).
35. M. I. Petrov, D. A. Balaev, S. V. Ospishchev, et al., *Phys. Lett. A* **237**, 85 (1997).
36. M. I. Petrov, D. A. Balaev, D. M. Gohfeld, et al., *Physica C* (Amsterdam) **314**, 51 (1999).
37. M. I. Petrov, D. A. Balaev, K. A. Shaikhutdinov, and K. S. Aleksandrov, *Fiz. Tverd. Tela* (St. Petersburg) **41**, 969 (1999) [*Phys. Solid State* **41**, 881 (1999)].
38. M. I. Petrov, D. A. Balaev, K. A. Shaikhutdinov, and K. S. Aleksandrov, *Supercond. Sci. Technol.* **14**, 798 (2001).
39. M. I. Petrov, D. A. Balaev, and K. A. Shaikhutdinov, *Physica C* (Amsterdam) **361**, 45 (2001).
40. K. A. Shaikhutdinov, D. A. Balaev, S. I. Popkov, and M. I. Petrov, *Fiz. Tverd. Tela* (St. Petersburg) **45**, 1776 (2003) [*Phys. Solid State* **45**, 1866 (2003)].
41. A. Barone and G. Paterno, *Physics and Applications of the Josephson Effect* (Wiley-Interscience, New-York, 1982; Mir, Moscow, 1984), p. 639.
42. A. D. Balaev, Yu. V. Boyarshinov, M. I. Karpenko, and B. P. Khrustalev, *Prib. Tekh. Éksp.*, No. 3, 167 (1985); Available from VINITI, No. 69-85.
43. D.-X. Chen, R. B. Goldfarb, R. W. Gross, and A. Sanchez, *Phys. Rev. B* **48**, 6426 (1993).
44. Y. M. Kim, C. F. Hempstead, and A. M. Strnad, *Phys. Rev.* **131**, 2486 (1963).
45. L. F. Cohen and H. J. Jensen, *Rep. Prog. Phys.* **60**, 1581 (1997).
46. G. Blatter, M. V. Feigel'man, V. B. Gekshkebein, et al., *Rev. Mod. Phys.* **66**, 1125 (1994).

*Translated by N. Wadhwa*